Greedy Selection of the Torso Electrodes for the Solution of Inverse Problem with a Single Dipole

[1,2]Beata Ondrusova, [1]Jana Svehlikova, [1]Milan Tysler, [3]Peter Tino

[1]Institute of Measurement Science, Slovak Academy of Sciences, Bratislava, Slovakia
[2]Faculty of Electrical Engineering and Information Technology, Slovak University of Technology, Bratislava, Slovakia
[3]School of Computer Science, The University of Birmingham, Birmingham, United Kingdom

Abstract

Many torso electrodes are used to solve the inverse problem of electrocardiography. We investigate which ones are the most important for the solution based on 4 different criteria. Body surface potential measurements in 128 and 192 electrodes from one patient-specific dataset (Bratislava) and two torso tank experimental datasets (Bordeaux, Utah) with the known position of the ventricular stimulation were used as a testbed to analyse solutions of the inverse problem with a single dipole. Electrode sets used for the solutions were constructed incrementally according to the singular value decomposition of the transfer matrix. Electrode sets were chosen for 4 optimality criteria: A) minimized condition number, B) maximized product of singular values, C) maximized sum of singular values and D) joint criterion of A and B. Starting from the initial set of 4 best electrodes, the electrode set was incrementally enlarged by a single electrode at a time in a greedy manner. The accuracy of the inverse solution was determined by the localization error (LE). For Bratislava, the best results were achieved for C and D, with LE decreasing to 7.1 mm (10% of electrodes) and 7.5 mm (13% of electrodes). The LE with all electrodes used was 16.0 mm, suggesting beneficial effects of the sparsity enforcement in the electrode space. For Bordeaux and Utah, the best results were obtained for A and C, with LE 10.91 mm (9% of electrodes) and 14.2 mm (11% of electrodes).

1. Introduction

In recent years, the solution of the inverse problem of electrocardiography called also electrocardiographic imaging (ECGI) has been a tool of interest due to its ability to non-invasively describe the electrical activity of the heart. To achieve this goal, body surface potentials (BSPs) need to be recorded and the patient-specific geometrical model of the thorax needs to be created [1]. The BSPs are recorded in multiple sites on the thorax to capture complex information about the surface potential distribution. Currently, multi-lead ECG measuring systems with 64 [2], 128 [3], or 256 [4] leads are used. However, using so many electrodes in a clinical setup is challenging. Therefore, researchers are investigating the number and positions of the electrodes on the thorax needed for the accurate solution of the ECGI [5]. Further, some electrodes may be detected as faulty, or signals from some electrodes are contaminated with a high level of noise. Thus, information on the significance of individual torso electrodes for the solution of the ECGI is needed.

In this study, we examine different torso electrode sets chosen by different optimality criteria and their impact on the solution of the ECGI. The preferable electrode sets were constructed incrementally according to the singular value decomposition (SVD) of the transfer matrix. Starting from the initial set of 4 best electrodes, the electrode set was incrementally enlarged by a single electrode at a time in a greedy manner for 4 different optimality criteria.

2. Data and Methods

The solution of the inverse problem describes the cardiac electrical source H using the equation

$$H = T^{+}\Phi, \quad (1)$$

where T^{+} is pseudoinverse of the transfer matrix and Φ is a vector of measured BSPs. The schematic overview of this study in which the inverse problem is solved using a selection of 4 up to the full number of electrodes (N) based on one of the four optimality criteria is depicted in Figure 1.

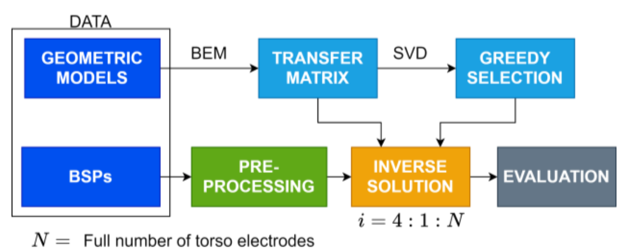

Figure 1. The schematic overview of the study pipeline.

Data: The BSP measurements in 128 and 192 electrodes from one patient-specific dataset (Bratislava-128) and two torso tank experimental datasets (Bordeaux-128, Utah-192) with the known position of the ventricular stimulation were used. Bratislava human mapping dataset was obtained by the Institute of Measurement Science, Slovak Academy of Sciences and the National Institute for Cardiovascular Diseases in Bratislava. The Bordeaux tank data were obtained by the Liryc-The Electrophysiology and Heart Modelling Institute in Bordeaux, France. The Utah tank data were obtained from the Scientific Computing and Imaging Institute in Salt Lake City, Utah. All datasets contain the BSPs, the geometric models of the heart ventricles and the torso surfaces in form of 3D triangle meshes and the coordinates of the pacing site.

Pre-processing: Cubic spline interpolation was used to remove baseline drift in measured ECG signals. Pan-Tompkins's algorithm was used for the detection of QRS complexes. The detected QRS complexes were clustered into those corresponding to the sinus rhythm and those corresponding to the paced beats using the *k*-means algorithm [6]. Paced beats in each lead were averaged and the body surface potential map Φ was computed from the beginning of the QRS complex up to 30 ms. During this short time interval, the activated area of the heart myocardium is small enough to be represented by a single dipole that is assumed as a cardiac source in this study.

Transfer matrix: The transfer matrix T reflects the relation between the cardiac electrical sources and potentials on the torso surface considering the patient-specific geometrical and electrical properties of the torso and internal organs. The observability of a given cardiac source by the electrodes on the torso surface is represented by the rows of the transfer matrix T. The transfer matrix T was computed using the boundary element method (BEM) assuming a single dipole as a cardiac electrical source that is located within the homogeneous volume conductor.

Greedy selection: The transfer matrix T can be written using SVD as

$$T = U\Sigma V^T, \tag{2}$$

where U and V are orthogonal matrices and Σ contains the square roots of eigenvalues of TT^T and T^TT on its diagonal and everywhere else are zeros. The singular values are sorted as

$$\sigma_1 > \sigma_2 > \sigma_3. \tag{3}$$

The selection of the torso electrodes for the solution of the inverse problem is based on the SVD of the transfer matrix T_{SD} computed for a true origin of the ventricular activity (pacing site). The dipole has three orthogonal components and thus the size of this transfer matrix T_{SD} is the number of electrodes $N \times 3$. We tested four optimality criteria.

The first criterion A minimizes the condition number computed as

$$A = {\sigma_1}/{\sigma_3}. \tag{4}$$

The second criterion B maximizes the product of singular values computed as

$$B = \sigma_1 * \sigma_2 * \sigma_3. \tag{5}$$

The third criterion C maximizes the sum of singular values computed as

$$C = \sigma_1 + \sigma_2 + \sigma_3. \tag{6}$$

The last criterion D represents the intersection of criteria A and B. Here, only the combinations of electrodes that satisfy both criteria to a high degree were chosen for the solution of the inverse problem.

The greedy algorithm was implemented in order to select torso electrodes for the solution of the inverse problem for each of the optimality criteria. First, the starting combination of 4 electrodes (4 rows of the transfer matrix T_{SD}) that met the optimality criterion best were chosen from all possible combinations K, where $K(128{,}4) = 10\,668\,000$ and $K(192{,}4) = 54\,870\,480$. The size of the chosen transfer matrix T_{SD} was 4×3. In the i following steps, the remaining electrodes were inspected. In each step, one electrode was added to the previously selected combination and thus the size of the transfer matrix T_{SD} at the i-th step was $(4 + i) \times 3$. The electrodes were chosen without replacement. In this greedy algorithm, we select the electrodes one-by-one in each step. We are not allowed to go back and revise our selection.

Inverse solution: Equation (1) was used to compute the solution of the inverse problem. The solution is searched for all possible positions of the single dipole – here the nodes of the cardiac surface. For the solution, 4 up to N rows (corresponding to the selected torso electrodes) of the transfer matrix T and potential map Φ were used. The dipole that best describes the electrical activity was chosen based on the criterion of the minimal relative residual error (RRE). The RRE was computed between the measured potential map Φ_M and the map Φ_C generated by the single dipole j in time instant t as

$$RRE(j,t) = \frac{\|\Phi_M(t) - \Phi_C(t)\|}{\|\Phi_M(t)\|}. \tag{7}$$

Evaluation: The accuracy of the inverse solution using 4 up to N electrodes is expressed as the localization error (LE). The minimal and maximal achievable LE was computed as the Euclidean distance between the pacing site (the true origin of ventricular activity) and the nearest and furthest node of the ventricular mesh. The LE of the solution was computed as the Euclidean distance between the pacing site and the position computed by the inverse solution. The range of the LE values is expressed as the Min-Max and Mode (the most often appearance) computed using 4 to $N/2$ and 4 to N electrodes.

3. Results

In this study, the inverse problem was solved using 4 up to N torso electrodes that were selected based on the chosen optimality criteria. First, the starting combination of 4 electrodes was selected for each criterion. Even though the chosen combination met the given criterion to the highest degree, other combinations could be just as good for the inverse task of transferring torso signals back to the source location. Figure 2 shows the position of electrodes that occurred most often in the 1% of the best 4-electrode combinations.

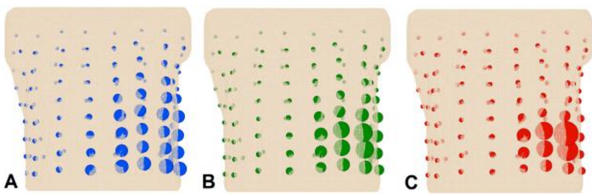

Figure 2: The occurrence of the electrodes within 1% of the best combinations of 4 electrodes for the Bratislava dataset. The size of the electrode corresponds to its occurrence.

The gradual addition of electrodes is depicted in Figure 3 for the Bratislava dataset. The starting combination of 4 electrodes is shown as black circles. In each subsequent step, one electrode was added (red to blue circles) for the solution of the inverse problem and the LE was computed. In each step, the electrode was selected so that the given criterion was met. The LE was 16.0 mm using 128 electrodes as shown in Table 1. For criterion A, good localization can be observed using a lower number of electrodes. However, there was no significant improvement in the LE when using a lower number of electrodes. The improvement of the LE can be observed for criteria B and C. For B, the best achieved LE was 7.1 mm and 7.5 mm. These LE were obtained when 7% up to 23% of electrodes were used. For C, the most stable results with the lowest LE of 7.1 mm were observed when 13% to 27% of electrodes were used. The value of criteria B and C increased after each step, but the rapid increase observed using a lower number of electrodes was followed by a slowdown. For criteria D, the LE of 7.5 mm was observed using from 10% to 28% of electrodes.

The LE computed for Bordeaux and Utah datasets is shown in Figure 4 for all criteria and a summary of the results is shown in Table 1. For all criteria, using up to 10 electrodes led to a high LE. Using more than 10 electrodes, the LE improved, and it was comparable to the LE computed using the full set of electrodes. However, slight improvement in the LE can be observed also for Bordeaux and Utah datasets.

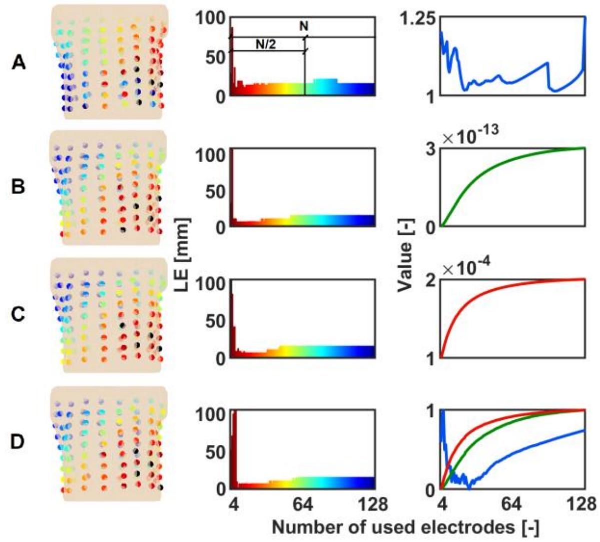

Figure 3: Left: The position of the torso electrodes used for the inverse solution (starting combination of 4 electrodes – black circles, gradually added electrodes – red to blue circles). Middle: The LE obtained using 4 up to 128 electrodes for the solution of the inverse problem. Right: The value of selected criteria in each step of the greedy algorithm. For criterion *D*, the values of criteria *A* (blue), *B* (green), and *C* (red) are scaled between 0 and 1. Note that the combinations of electrodes are different for each criterion.

Table 1: The minimal and maximal achievable LE, the minimal and maximal LE obtained using 4 up to N electrodes, the Mode for 4 up to $N/2$ and 4 up to N electrodes and LE for the full set of electrodes. The values are in mm.

Criteria	Min-Max	Mode for *N*/2	Mode for *N*	Full set
Bratislava (Min-Max achievable LE =1.6 - 134.1)				
A	11.2-86.8	16.0	16.0	16.0
B	7.1-109.0	11.2	16.0	16.0
C	7.1-104.8	7.1	16.0	16.0
D	1.6-104.8	7.5	16.0	16.0
Bordeaux (Min-Max achievable LE = 1.5 - 79.5)				
A	9.0-67.1	12.3	12.5	12.5
B	12.3-67.7	12.3	12.5	12.5
C	12.3-76.2	12.3	12.3	12.5
D	12.3-77.9	12.5	12.3	12.5
Utah (Min-Max achievable LE = 4.2 - 62.0)				
A	6.8-53.3	26.1	22.1	18.0
B	14.2-59.6	18.0	18.0	18.0
C	14.1-49.3	14.2	18.0	18.0
D	4.2-47.3	18.0	18.0	18.0

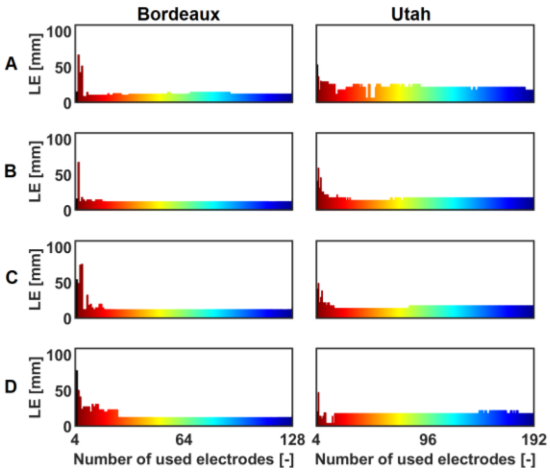

Figure 4: The LE obtained using 4 up to N electrodes for the solution of the inverse problem for all criteria.

4. Discussion and conclusion

By the greedy selection of the torso electrodes, the electrodes from the same area were selected for all criteria. For the Bratislava dataset (Figure 2, Figure 3), it started with the electrodes in the lower left half of the anterior chest that is located closest to the pacing site, and it ended with those in the area of the right shoulder.

Further, it was shown that not all torso electrodes are needed for an accurate solution of the inverse problem. Similar or more accurate localizations can be obtained using a lower number of electrodes compared to the full set as was shown for the Bratislava (criteria *B*, *C*, *D*), Bordeaux (criteria *A*, *B*, *C*) and Utah dataset (*C*) (Table 1). However, the most significant improvement of the LE was observed for the Bratislava dataset (Table 1). Compared to the other datasets, this is a more complex patient-specific dataset and thus the electrodes without the “proper view” of the heart could bring uncertainty to the solution of the inverse problem. The first criterion A minimizes the condition number that shows how well the given matrix can be inverted. The minimal values of condition numbers were close to 1. That suggests that the transfer matrix computed using a chosen combination of electrodes is considered to be well invertible. As shown in Figure 3, the values fluctuated between steps because of the greedy selection that does not optimize previous steps. This criterion omits the second singular σ_2 compared to the other criteria and thus slightly different results could be observed. The second criterion B maximizes the product of singular values. This criterion represents the volume characteristics. The third criterion C maximizes the sum of singular values and represents the total variance. For criteria *B* and *C*, similar electrodes were chosen gradually for the solution of the inverse problem which is in line with their similar interpretation. The last criterion represents the intersection of criteria A and B. The transfer matrices used for the solution satisfied the condition of the minimal condition number as well as the maximized multiplication of singular values. The electrodes were added very similarly to the solution as in the case of criteria B and C. This approach increased computational demands while the results were similar.

It was shown that accurate localization could be obtained using a lower number of electrodes that were selected based on one of the criteria for the known position of the origin of ventricular activity. The limitation of the study is that the combinations of electrodes were chosen for the known position of the origin of the ventricular activity without analysis of measured signals. Another limitation is that we did not investigate how many electrodes are needed for an accurate solution. To overcome these limitations, the measured signals and the course of the criteria curve should be investigated and subsequently, a two-step inverse solution should be implemented.

Acknowledgments

The authors would like to thank the IHU Liryc, France and the SCI Institute in Salt Lake City, Utah for providing the data. The presented work was supported by the VEGA Grant Agency under grant number 2/0109/22, by the Slovak Research and Development Agency under grant number APVV-19-0531 and by the Slovak Academy of Sciences under grant number APP0323.

References

[1] M. J. M. Cluitmans, R. L. M. Peeters, R. L. Westra, and P. G. A. Volders, “Noninvasive reconstruction of cardiac electrical activity: Update on current methods, applications and challenges,” *Netherlands Hear. J.*, vol. 23, no. 6, pp. 301–311, 2015.

[2] P. Oosterhoff et al., “Experimental validation of noninvasive epicardial and endocardial activation imaging,” *Circ. Arrhythmia Electrophysiol.*, vol. 9, no. 8, pp. 1–11, 2016.

[3] J. Kadanec, J. Zelinka, G. Bukor, and M. Tyšler, “ProCardio 8 - System for high resolution ECG mapping,” in *MEASUREMENT*, 2017, pp. 263–266.

[4] L. R. Bear et al., “Advantages and pitfalls of noninvasive electrocardiographic imaging,” *J. Electrocardiol.*, vol. 57, pp. S15–S20, 2019.

[5] D. D. Finlay et al., “Selection of optimal recording sites for limited lead body surface potential mapping: A sequential selection based approach,” *BMC Med. Inform. Decis. Mak.*, vol. 6, no. 1, pp. 1–9, Feb. 2006.

[6] J. Svehlikova et al. “Influence of individual torso geometry on inverse solution to 2 dipoles,” *J. Electrocardiol.*, vol. 45, no. 1, pp. 7–12, 2012.

Address for correspondence:

Beata Ondrusova
Dubravska cesta 9, 841 01, Bratislava, Slovakia
beata.ondrusova@savba.sk